J|A|C|S ARTICLES

Published on Web 03/10/2010

Electronic Tuning of Two Metals and Colossal Magnetoresistances in $EuWO_{1+x}N_{2-x}$ Perovskites

Minghui Yang,[†] Judith Oró-Solé,[‡] Anna Kusmartseva,[†] Amparo Fuertes,*[,‡] and J. Paul Attfield*[,†]

Centre for Science at Extreme Conditions and School of Chemistry, University of Edinburgh, King's Buildings, Mayfield Road, Edinburgh, EH9 3JZ, United Kingdom, and Institut de Ciència de Materials de Barcelona (CSIC), Campus U.A.B., 08193 Bellaterra, Spain

Received December 21, 2009; E-mail: amparo.fuertes@icmab.es; j.p.attfield@ed.ac.uk

Abstract: A remarkable electronic flexibility and colossal magnetoresistance effects have been discovered in the perovskite oxynitrides $EuWO_{1+x}N_{2-x}$. Ammonolysis of $Eu_2W_2O_9$ yields scheelite-type intermediates $EuWO_{4-y}N_y$ with a very small degree of nitride substitution ($y = 0.04$) and then $EuWO_{1+x}N_{2-x}$ perovskites that show a wide range of compositions $-0.16 \leq x \leq 0.46$. The cubic lattice parameter varies linearly with x, but electron microscopy reveals a tetragonal superstructure. The previously unobserved $x < 0$ regime corresponds to oxidation of Eu (hole doping of the Eu:4f band), whereas $x > 0$ materials have chemical reduction of W (electron doping of the W:5d band). Hence, both the Eu and W oxidation states and the hole/electron doping are tuned by varying the O/N ratio. $EuWO_{1+x}N_{2-x}$ phases order ferromagnetically at 12 K, and colossal magnetoresistances (CMR) are observed in the least doped ($x = -0.04$) sample. Distinct mechanisms for the hole and electron magnetotransport regimes are identified.

Introduction

Transition metal oxynitrides are an important class of emerging materials that in optimal cases may combine the advantages of transition metal oxides and nitrides. They generally have greater air and moisture stability than pure nitrides, but with smaller bandgaps than comparable oxides, leading to useful electronic or optical properties. Nitrogen doping of TiO_2 tunes the bandgap from the UV to the visible region for photocatalysis,[1] and stoichiometric oxynitrides such as TaON[2] also have photocatalytic applications. Oxynitrides of lithium and light transition elements have been reported as anode materials for rechargeable lithium batteries, showing high reversibility and capacity as well as enhanced chemical stability with respect to nitrides.[3] Quaternary transition metal oxynitride perovskites synthesized by ammonolysis[4,5] or high-pressure reactions[6] show a range of properties; for example, $CaTaO_2N$-$LaTaON_2$ solid solutions are nontoxic red-yellow pigments,[7] $BaTaO_2N$ has a high dielectric constant[8] and photocatalyzes the decomposition of water,[9] and $EuNbO_2N$ is ferromagnetic and shows colossal magnetoresistances (CMR).[10]

The study of $EuNbO_2N$ and $EuTaO_2N$ was motivated by the possibility of discovering new multiferroic materials in which ferromagnetic and ferroelectric polarizations are coupled.[10] These are attractive candidates, as ferromagnetic order of the $4f^7$ $S = 7/2$ spins is observed in many Eu^{2+} compounds, e.g., EuO, while the "off-center" instabilities of d^0 transition metal cations can generate large ferroelectric polarizations, e.g., in $BaTiO_3$ and $LiNbO_3$, and any O^{2-}/N^{3-} anion order could help to align the displacements of neighboring cations. However, no intrinsic ferroelectric effects were observable, as these materials were found to be electronically doped through slight deviations from stoichiometry. Careful synthetic control of the O/N ratio is thus important for tuning the materials properties of such oxynitrides, in particular when mixed oxidation states are present. Oxide and nitride may substitute for one another in many solid-state structures if a compensating redox mechanism is available, and so chemical analysis is required to check how closely sample compositions correspond to stoichiometric oxynitride formulas.

The discovery of CMR in $EuNbO_2N$ resulted from a slight nitrogen deficiency leading to electron doping of the Nb d-band (reduction of Nb^{5+} to Nb^{4+}), as the coupling of the carrier spins to those of the localized, ferromagnetically ordered Eu^{2+} $S = 7/2$ states gives rise to colossal magnetoresistances at low temperatures (>99% reduction of resistance at 2 K).[10] Materials showing CMR are of interest for memory and sensor applica-

[†] University of Edinburgh.
[‡] Institut de Ciència de Materials de Barcelona.

(1) Asahi, R.; Morikawa, T.; Ohwaki, T.; Aoki, K.; Taga, Y. *Science* **2001**, *293*, 269–271.
(2) Hitoki, G.; Takata, T.; Kondo, J. N.; Hara, M.; Kobayashi, H.; Domen, K. *Chem. Commun.* **2002**, 1698–1699.
(3) Cabana, J.; Rousse, G.; Fuertes, A.; Palacín, M. R. *J. Mater. Chem.* **2003**, *13*, 2402–2404.
(4) Marchand, R.; Pors, F.; Laurent, Y. *Rev. Int. Hautes Temp. Refract. Fr.* **1986**, *23*, 11–15.
(5) Tobías, G.; Oró-Solé, J.; Beltrán-Porter, D.; Fuertes, A. *Inorg. Chem.* **2001**, *40*, 6867–6875.
(6) Yang, M.; Rodgers, J. A.; Middler, L. C.; Oró-Solé, J.; Jorge, A. B.; Fuertes, A.; Attfield, J. P. *Inorg. Chem.* **2009**, *48*, 11498–11500.
(7) Jansen, M.; Letschert, H. P. *Nature* **2000**, *404*, 980–982.
(8) Kim, Y.; Woodward, P. M.; Baba-Kishi, K. Z.; Tai, C. W. *Chem. Mater.* **2004**, *16*, 1267–1276.
(9) Highashi, M.; Abe, R.; Takata, T.; Domen, K. *Chem. Mater.* **2009**, *21*, 1543–1549.
(10) Jorge, A. B.; Oró-Solé, J.; Bea, A. M.; Mufti, N.; Palstra, T. T. M.; Rodgers, J. A.; Attfield, J. P.; Fuertes, A. *J. Am. Chem. Soc.* **2008**, *130*, 12572–12573.

 10.1021/ja910745b

tions, and large magnetoresistances had not previously been reported in oxynitrides, so we have investigated the perovskite reported in the Eu−W−O−N system.[11] A preliminary study showed that giant magnetoresistances (up to 70% loss of resistance) and non-ohmic conductivity were observed at low temperatures in nitrogen-deficient $EuWO_{1+x}N_{2-x}$ samples with $0.09 < x < 0.25$.[12] The significant compositional range found in our initial samples has prompted a full study of the chemistry and magnetoresistive properties of the $EuWO_{1+x}N_{2-x}$ system that is reported here. This has revealed a remarkable electronic flexibility, as the oxidation states of both metals can be tuned by varying the O/N ratio, enabling hole- and electron-doped regimes to be accessed and the discovery of colossal magnetoresistances close to $x = 0$.

Experimental Section

An $Eu_2W_2O_9$ precursor was prepared by a solid-state reaction between Eu_2O_3 (99.99%, Aldrich) and WO_3 (99.99%, Aldrich), which were heated for three 24 h periods at temperatures of 950 to 1150 °C with intermediate regrindings. Samples (0.2−0.3 g) of $Eu_2W_2O_9$ were placed in an alumina boat in a tube furnace for ammonolysis. Nitrogen gas (oxygen-free, BOC) was passed over the sample for 15 min to expel air before the flow of ammonia gas (99.999%, BOC) was started. The sample was heated to the reaction temperature at 150 °C/h and furnace cooled after treatment. Sintered pellets were prepared for resistivity measurements by heating compressed $EuWO_{1+x}N_{2-x}$ powders at 550 °C for 3 h under ammonia gas flowing at 250 cm^3 min^{-1}.

The nitrogen contents of the products were determined as N_2 by a combustion method using a Carlo Erba CHNS analyzer. Approximately 3 mg of finely ground powder was used for each analysis, and results of three analyses were averaged for each sample. Finely ground powders were examined with a Bruker D8 Advance powder X-ray diffractometer with monochromatic Cu $K\alpha_1$ radiation ($\lambda = 1.540562$ Å). Scans were taken in the 2θ range 10−120° with a 0.007° step size and a 3s count time. Crystal structures were fitted to the X-ray diffraction profiles using the GSAS package.[13] Electron diffraction micrographs were obtained in a JEOL 1210 transmission electron microscope operating at 120 kV, equipped with a side-entry 60/30° double tilt GATHAN 646 specimen holder. The samples were prepared by dispersing the powders in ethanol and depositing of a droplet of this suspension on a carbon-coated holey film supported on a copper grid.

Electrical resistivities were measured from 2 to 300 K in 0 and 7 T magnetic fields using a four-probe method with a Quantum Design Physical Properties Measurement System. Resistivity-field measurements were made at 2, 8, 15, 30, and 50 K by varying the magnetic field between −7 and +7 T. Magnetic susceptibilities were recorded using a Quantum Design Magnetic Properties Measurement System SQUID magnetometer under an external field of 100 Oe from 2 to 300 K after cooling the sample in the field (FC) or in zero field (ZFC). Magnetization-field loops were measured between −7 and +7 T at 2, 8, 15, 30, and 50 K.

Results and Discussion

(a) Ammonolysis of $Eu_2W_2O_9$. $Eu_2W_2O_9$ is a convenient precursor for the ammonolytic synthesis of $EuWO_{1+x}N_{2-x}$, as it provides a 1:1 atomic scale mixture of Eu and W. Impure samples of this precursor were found to give impure perovskite products, so the X-ray diffraction profile was fitted to check for the presence of secondary phases. The $Eu_2W_2O_9$ sample used in the reactions below was white in color and gave refined cell parameters $a = 7.5535(1)$ Å, $b = 9.6769(2)$ Å, $c = 9.1226(2)$ Å, $\beta = 107.76(2)°$ in space group $P2_1/c$, in agreement with published data,[14] and with no additional phases observed.

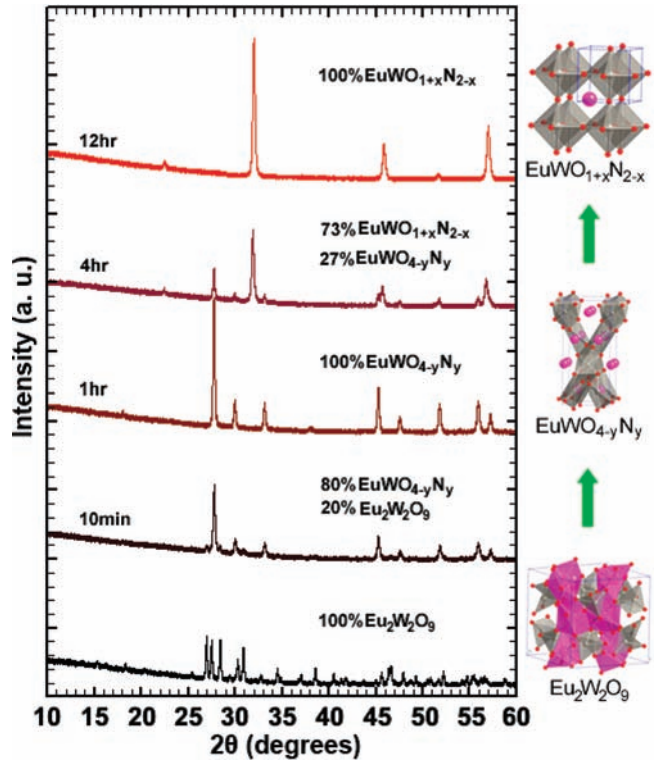

Figure 1. Powder X-ray diffraction patterns illustrating the conversion of $Eu_2W_2O_9$ to the perovskite $EuWO_{1+x}N_{2-x}$ via an intermediate scheelite phase $EuWO_{4-y}N_y$, with the crystal structures also shown. The ammonolysis was performed at 600 °C with a flow rate of 250 cm^3 min^{-1}.

Ammonolysis reactions of this precursor were carried out for a range of temperatures (450−850 °C), ammonia flow rates (22 to 250 cm^3 min^{-1}), and times (10 min to 12 h) to explore the reaction pathway and compositional variations in the products. The reaction was found to proceed via a crystalline, scheelite ($CaWO_4$)-type intermediate phase, of ideal composition $EuWO_4$, as shown by the representative powder X-ray diffraction patterns in Figure 1. Ammonia can act as a simultaneous reducing and nitriding agent or can bring about just one of these changes. In this case, the reaction proceeds through two distinct steps, which in the simplest description are a reduction and a nitride substitution according to the ideal formulas:

$$Eu_2^{3+}W_2^{6+}O_9 \rightarrow Eu^{2+}W^{6+}O_4 \rightarrow Eu^{2+}W^{6+}ON_2$$

However, a range of Eu and W redox states is found for the final perovskite product, as discussed later. No additional amorphous X-ray scattering is observed during the conversions of $Eu_2W_2O_9$ to $EuWO_4$ and of $EuWO_4$ to the perovskite phase (see the two two-phase patterns in Figure 1). This demonstrates that the reduction of $Eu_2W_2O_9$ and nitridation of $EuWO_4$ reactions are each followed by rapid recrystallization, as there are no simple topotactic relations between the $Eu_2W_2O_9$, $EuWO_4$, and perovskite structures.

(11) Pastrana-Fabregas, R.; Isasi-Marin, J.; Cascales, C.; Saez-Puche, R. *J. Solid State Chem.* **2007**, *180*, 92–97.
(12) Kusmartseva, A.; Yang, M.; Oró-Solé, J.; Bea, A. M.; Fuertes, A.; Attfield, J. P. *Appl. Phys. Lett.* **2009**, *95*, 022110.
(13) Larson, A. C.; Von Dreele, R. B. *General Structure Analysis System (GSAS)*; Los Alamos National Laboratory Report LAUR; **1994**, pp 86−748.
(14) MaCarthy, G. J.; Fischer, R. D.; Sanzgiri, J. *J. Solid State Chem.* **1971**, *5*, 200–206.

Table 1. Reaction Conditions (ammonia flow rate = 250 cm^3 min^{-1}) and Lattice Parameters for the Scheelite Phases $EuWO_{4-y}N_y$ Formed by the Ammonolysis of $Eu_2W_2O_9$, with the Reported Lattice Parameters[14] for $EuWO_4$ Shown for Comparison in the Final Row

temperature/°C	time/h	*a*/Å	*c*/Å	*V*/Å^3
450	12	5.4078(1)	11.9362(2)	349.07(1)
500	12	5.4130(1)	11.9503(3)	350.15(2)
550	12	5.4144(1)	11.9511(1)	350.36(1)
600[a]	4	5.4140(1)	11.9547(6)	350.42(2)
		5.411(1)	11.936(1)	349.4(1)

[a] This sample contains both scheelite and perovskite phases, as shown in Figure 1.

(b) Synthesis of $EuWO_{4-y}N_y$ Scheelites. Ammonolyses at temperatures between 450 and 550 °C produced single-phase samples of the tetragonal scheelite intermediate with ideal composition $EuWO_4$. This structure contains eight-coordinate Eu^{2+} and isolated tetrahedral tungstate groups. Reaction conditions and lattice parameters for the resulting samples and those reported for $EuWO_4$[14] are shown in Table 1, and the profile fit and structural results are in the Supporting Information. Small variations in the unit cell parameters between samples indicate that these scheelites are slightly nonstoichiometric.

Eu-deficient scheelite phases $Eu_{1-x}WO_4$ ($0 < x < 0.18$) in which oxidation of Eu^{2+} to Eu^{3+} is compensated by cation deficiency, i.e., $Eu^{2+}{}_{1-3x}Eu^{3+}{}_{2x}WO_4$, are known, but these show a contraction of the cell parameters with increasing x.[14] Our scheelite samples obtained from ammonolyses at 500−600 °C show expansion of the unit cell relative to that of $EuWO_4$, indicating that a different mechanism is present. A likely explanation is that the oxidation of Eu^{2+} is compensated by nitride substitution, i.e., $Eu^{2+}{}_{1-y}Eu^{3+}{}_yWO_{4-y}N_y$, and chemical analysis of the 550 °C sample in Table 1 showed that 0.13(1) wt % N is present, corresponding to a value of $y = 0.04$. This small N content is consistent with the average Eu−O(/N) bond distance of 2.62 Å, which is in good agreement with the ideal Eu^{2+}−O distance of 2.61 Å predicted from ionic radii. These samples also show a change in color, from off-white to orange, as the ammonolysis temperature increases (see photograph in Supporting Information). This is consistent with a shift of bandgap or the introduction of additional optical absorptions associated with the nitride doping.

Stoichiometric, scheelite-type oxynitrides $LnWO_3N$ have previously been obtained by ammonolysis of $Ln_2W_2O_9$ for the trivalent lanthanides Ln = La, Sm, Nd, and Dy,[15] but the Eu analogue, corresponding to the $y = 1$ limit of $Eu^{2+}{}_{1-y}Eu^{3+}{}_yWO_{4-y}N_y$, was not obtained. $EuWO_3N$ would be a plausible intermediate if a nitridation reaction occurred before reduction, i.e.,

$$Eu_2^{3+}W_2^{6+}O_9 \rightarrow Eu^{3+}W^{6+}O_3N \rightarrow Eu^{2+}W^{6+}ON_2$$

but our results show that almost complete reduction occurs before nitridation, so the $Eu^{2+}{}_{1-y}Eu^{3+}{}_yWO_{4-y}N_y$ phase is formed only with small values of $y \approx 0.04$.

(c) Synthesis of $EuWO_{1+x}N_{2-x}$ Perovskites. The ammonolysis of $Eu_2W_2O_9$ at temperatures between 600 and 850 °C at various flow rates and reaction times (Table 2) produced pure phases of the perovskite $EuWO_{1+x}N_{2-x}$. Although the transformation from the scheelite phase to the ideal, $x = 0$, perovskite is not a redox reaction, the results show that this step proceeds via an initial reduction of W and nitride substitution to $EuWO_{1+x}N_{2-x}$ with $x \approx 0.5$, i.e., $Eu^{2+}W^{6+}{}_{0.5}W^{5+}{}_{0.5}O_{1.5}N_{1.5}$, followed by reoxidation during further reaction as x decreases. Systematic investigations of the effects of temperature or ammonia flow rate on the nitrogen content are shown in Figure 2. These demonstrate that either variable can be used to access a wide range of compositions within the domain of conditions used here. High temperatures and flow rates and long reaction times increase the nitrogen content.

Table 2. Ammonolysis Conditions for the Formation of $EuWO_{1+x}N_{2-x}$ Perovskites with Cubic Lattice Parameters and Analyzed Compositions x Shown

temperature/°C	flow rate/cm^3 min^{-1}	duration/h	*a*/Å	*x*
600	120	6	3.9779(3)	0.46
600	120	8	3.9756(2)	0.41
750	250	8	3.9674(1)	0.25
800	250	8	3.9621(1)	0.17
800	120	10	3.9591(1)	0.09
800	250	10	3.9556(2)	−0.04
850	120	10	3.9536(1)	−0.12
850	250	12	3.9472(2)	−0.16

Chemical analyses showed that a wide range of nitrogen contents ($-0.16 \le x \le 0.46$) were obtained. A notable discovery is that ammonolysis at relatively high temperatures of 800−850 °C gave nitrogen-rich materials with negative values of x in the $EuWO_{1+x}N_{2-x}$ formulation. Previous studies[11,12] reported only nitrogen-deficient materials with positive x values, corresponding to chemical reduction of W (electron doping of the W:5d(t_{2g}) band), formally $Eu^{2+}W^{6+}{}_{1-x}W^{5+}{}_xO_{1+x}N_{2-x}$. Our work demonstrates that materials in which Eu is oxidized (hole doping of the Eu:4f band) can also be accessed with formal compositions $Eu^{2+}{}_{1+x}Eu^{3+}{}_{1-x}W^{6+}O_{1+x}N_{2-x}$ for negative x values up to $x = -0.16$ in the present study. Hence, both the W and Eu oxidation states can be tuned in the $EuWO_{1+x}N_{2-x}$ system by varying the O/N ratio. The ideal $x = 0$ stoichiometry $EuWON_2$ does not appear to have any special chemical stability, and an attempt to prepare this composition resulted in a slightly N-rich ($x = -0.04$) sample.

All of the $EuWO_{1+x}N_{2-x}$ samples appear cubic by powder X-ray diffraction, and the patterns are fit well by the simple cubic $Pm\bar{3}m$ perovskite structure model with no superstructure peaks evident (see Supporting Information). The cubic lattice parameters (Table 2) show a linear variation with the analyzed

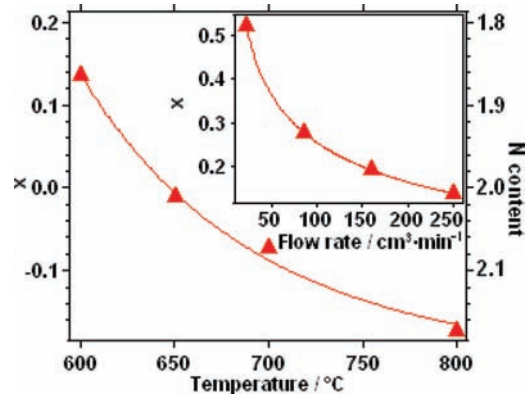

Figure 2. Plots of the compositional variable x for $EuWO_{1+x}N_{2-x}$ perovskites synthesized under ammonia at a flow rate of 250 cm^3 min^{-1} for 12 h at various temperatures and (inset) heated at 600 °C for 12 h at variable flow rates.

(15) Antoine, P.; Marchand, R.; Laurent, Y. *Rev. Int. Hautes Temp. Refract. Fr.* **1987**, *24*, 43–46.

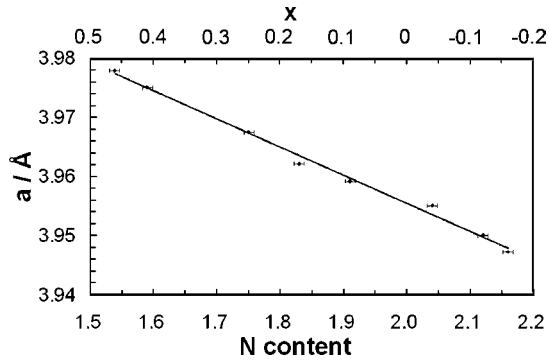

Figure 3. Plot of the cubic lattice parameter *a* against the analyzed N content and the equivalent variable *x* for $EuWO_{1+x}N_{2-x}$ samples.

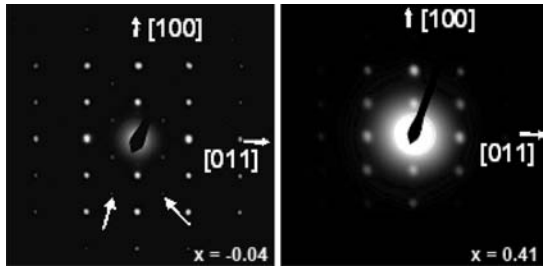

Figure 4. Electron diffraction patterns of representative crystallites of $EuWO_{1+x}N_{2-x}$ samples with $x = -0.04$ and 0.41. Additional spots that reveal a $\sqrt{2} \times \sqrt{2} \times 2$ body-centered superstructure in the former sample are marked by arrows.

nitrogen content for all samples (Figure 3), and no change in slope is evident at the $x = 0$ crossover between electron- and hole-doped regimes. The decrease in lattice parameter with increasing N content shows that the lattice contraction from the oxidations of the cations outweighs the expanding effect of replacing oxide by the larger nitride anion.[16]

The $EuWO_{1+x}N_{2-x}$ perovskites do not show any immediate degradation in air. However, after being stored in a stoppered vial for 32 weeks, the cubic lattice parameter of a nitrogen-rich sample was found to have increased by $\Delta a = 0.0223$ Å, equivalent to a composition change of $\Delta x = -0.47$ using the linear relationship in Figure 3. This shows that a slow substitution of nitride by oxide had occurred through reaction with atmospheric moisture or oxygen.

Superstructures are evident in the electron diffraction patterns of individual $EuWO_{1+x}N_{2-x}$ crystallites, as shown in Figure 4 and the Supporting Information. These contain additional reflections characteristic of a tetragonal $\sqrt{2} \times \sqrt{2} \times 2$ body-centered perovskite superstructure for the N-rich $x = -0.04$ and -0.12 samples. This superstructure was also observed in the previously reported $x = 0.09$ and 0.25 samples[12] and in the $EuNbO_2N$ and $EuTaO_2N$ analogues,[10] but it is notably absent for the most nonstoichiometric, $x = 0.41$ sample. Powder neutron diffraction studies of $SrNbO_2N$[17] and $SrTaO_2N$[18,19] have shown that a tetragonal $\sqrt{2} \times \sqrt{2} \times 2$ body-centered superstructure results from octahedral tilting with partial anion order in most refinements. It is likely that such superstructures are also formed in $EuWO_{1+x}N_{2-x}$, although the high degree of disorder present for the $x = 0.41$ sample suppresses the octahedral tilting transition to below room temperature. Neutron diffraction will be needed to resolve the superstructure, although the large neutron absorption cross-section of Eu may make such studies difficult. It is likely that significant O/N disorder is present in $EuWO_{1+x}N_{2-x}$, and there is evidence of disorder effects in the magnetic measurements below.

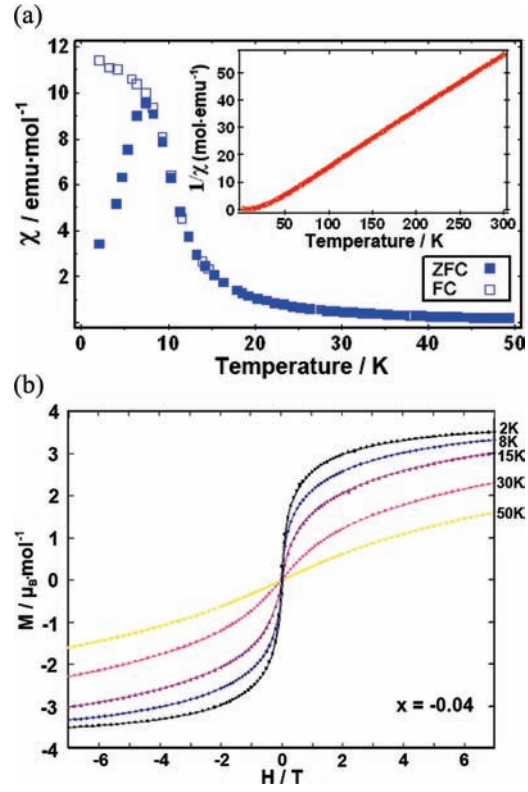

Figure 5. Magnetic measurements for $EuWO_{1.96}N_{2.04}$: (a) zero-field-cooled (ZFC) and field-cooled (FC) ac magnetic susceptibilities at low temperatures and the inverse FC susceptibility (inset), using a 0.01 T magnetic field; (b) magnetization-field loops.

(d) Magnetic and Electronic Properties of $EuWO_{1+x}N_{2-x}$ Perovskites. The magnetic, conductivity, and magnetoresistance properties of three $EuWO_{1+x}N_{2-x}$ samples with $x = 0.41$, -0.04, and -0.12 were measured to explore the effects of a large nitrogen deficiency and the new nitrogen-rich regime, in comparison to previously reported results for nitrogen-deficient $x = 0.09$, 0.17, and 0.25 samples.[12]

The magnetic susceptibilities of the samples have very similar temperature variations. All show a ferromagnetic transition at a Curie temperature of $T_C = 12 \pm 1$ K, below which field- and zero-field-cooled susceptibilities diverge (Figure 5). The high-temperature susceptibilities follow a Curie−Weiss variation, and the derived Curie constants, paramagnetic moments, and Weiss temperatures are shown in Table 3. The positive Weiss temperatures confirm the dominant ferromagnetic exchange interactions, and the maximum value is obtained for the $x = -0.04$ sample, which may signify higher structural order or loss of competing antiferromagnetic interactions at $x = 0$. Magnetization-field loops show typical behavior for soft ferromagnets at low temperatures, and the saturated magnetizations (taken from the 2 K data) are also shown in Table 3.

In the electron-doped ($x > 0$) regime, the formal valence distribution is $Eu^{2+}W^{6+}{}_{1-x}W^{5+}{}_xO_{1+x}N_{2-x}$, so the magnetic mo-

(16) Shannon, R. D. *Acta Crystallogr. A* **1976**, *32*, 751–767.
(17) Ebbinghaus, S. G.; Weidenkaff, A.; Rachel, A.; Reller, A. *Acta Crystallogr. C* **2004**, *60*, i91–i93.
(18) Clarke, S. J.; Hardstone, K. A.; Michie, C. W.; Rosseinsky, M. J. *Chem. Mater.* **2002**, *14*, 2664–2669.
(19) Gunther, E.; Hagenmayer, R.; Jansen, M. *Z. Anorg. Allg. Chem.* **2000**, *626*, 1519–1525.

Table 3. Results of Magnetic Measurements for $EuWO_{1+x}N_{2-x}$ Perovskites ($x = 0.41$, -0.04, and -0.12), Showing the Curie Constants, Effective Paramagnetic Moments, Weiss Temperatures, Saturated Moments at 2 K, and Curie Temperatures

x	0.41	−0.04	−0.12
C/emu K mol^{-1}	6.04	4.90	5.00
μ_{eff}/μ_B	6.96	6.27	6.34
θ/K	12.9	22.1	12.8
μ_{sat}/μ_B	5.48	3.50	3.38
T_C/K	12.3	11.3	11.5

ments are predicted to be close to the spin-only values of $\mu_{eff} = 7.9\ \mu_B$ and $\mu_{sat} = 7.0\ \mu_B$ for $S = 7/2$ Eu^{2+}. However, the hole-doped ($x < 0$) materials have the nominal distribution $Eu^{2+}{}_{1+x}Eu^{3+}{}_{1-x}W^{6+}O_{1+x}N_{2-x}$. Eu^{3+} has a nonmagnetic ($J = 0$) ground state, and although higher J states are thermally accessible, the moments become very small at low temperatures. Hence, the average Eu magnetic moments are expected to decrease in the hole-doped region. This trend is borne out by the data in Table 3, as the hole-doped materials have smaller paramagnetic and saturated moments than those for the electron-doped $x = 0.41$ sample and the previously reported $x = 0.17$ sample, which has $\mu_{sat} = 4.1\ \mu_B$, although there is little difference between the values for the $x = -0.04$ and -0.12 materials. All of the moments are below the predicted values, showing that more Eu^{3+} is present than expected from the chemical compositions. This evidences a significant influence of anion disorder on the electronic configurations. An ideal, anion-ordered, $x = 0$ composition $EuWON_2$ would be expected to contain only Eu^{2+} and W^{6+} states, but anion disorder can create nitride-rich regions that stabilize oxidation of Eu^{2+} to Eu^{3+}, balanced by oxide-rich regions where W^{6+} is reduced to W^{5+}. Hence, inhomogeneity in the anion distribution controls the internal redox equilibrium:

$$Eu^{2+} + W^{6+} \Leftrightarrow Eu^{3+} + W^{5+}$$

This reduces the magnetic moments by oxidizing Eu^{2+} to Eu^{3+} and creates electron−hole pairs that may affect the electronic transport and measured dielectric properties.

Another possible cause for the reduction of saturated magnetic moments in $EuWO_{1+x}N_{2-x}$ is the coexistence of ferromagnetically and antiferromagnetically ordered regions. The related oxide material $EuTiO_3$ is antiferromagnetic in zero field but converts to a full ferromagnetic order in fields above 1.5 T.[20] This might occur in $EuWO_{1+x}N_{2-x}$, but the magnetization-field loops (Figure 5b) show no evidence for such a change at low fields. Furthermore, the saturated moments are measured in a 7 T field and so are insensitive to any low-field antiferromagnetism. Hence anion disorder effects are the likely cause for the reduced moments.

The three measured samples all show semiconducting behavior (see Supporting Information), although the heavily doped $x = 0.41$ sample has relatively little temperature dependence and is approaching metallic conductivity. Anion disorder leading to the trapping of carriers (Anderson localization) may be responsible for the nonmetallic behavior at such high electron dopings, as similar doping levels in tungsten oxides introduce metallicity, e.g., in Na_xWO_3 bronzes.

The zero-field and 7 T resistivities diverge at low temperatures, signifying the onset of significant negative magnetoresistance effects (Figure 6). Field-dependent measurements of the negative magnetoresistance $-MR = (\rho_0 - \rho_H)/\rho_0$, where ρ_0 and ρ_H are the resistivities in zero- and applied-field H, respectively, are shown in Figure 7. The $x = 0.41$ and the hole-doped −0.12 samples both show large magnetoresistances, approaching −50 and −70% at 2 K in a 7 T field, similar to those for previously reported electron-doped $EuWO_{1+x}N_{2-x}$ materials.[12] However, the $x = -0.04$ sample shows much larger CMR effects with $-MR > 99\%$ at low temperatures. The maximum measurable value of $-MR$ was 99.7% at 7 K in a 7

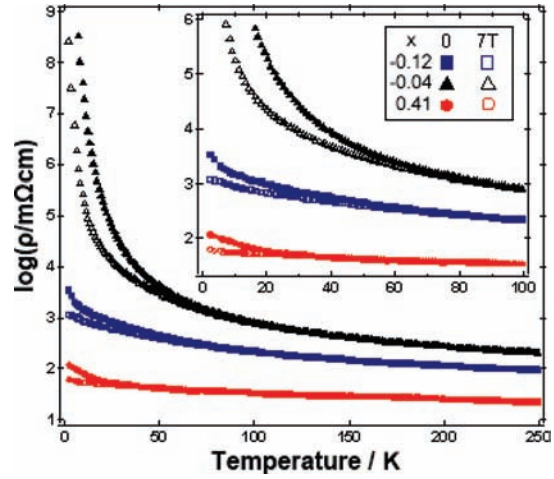

Figure 6. Temperature dependence of the electronic resistivities of $EuWO_{1+x}N_{2-x}$ ($x = 0.41$, -0.04, and -0.12) in zero field and in a magnetic field of 7 T.

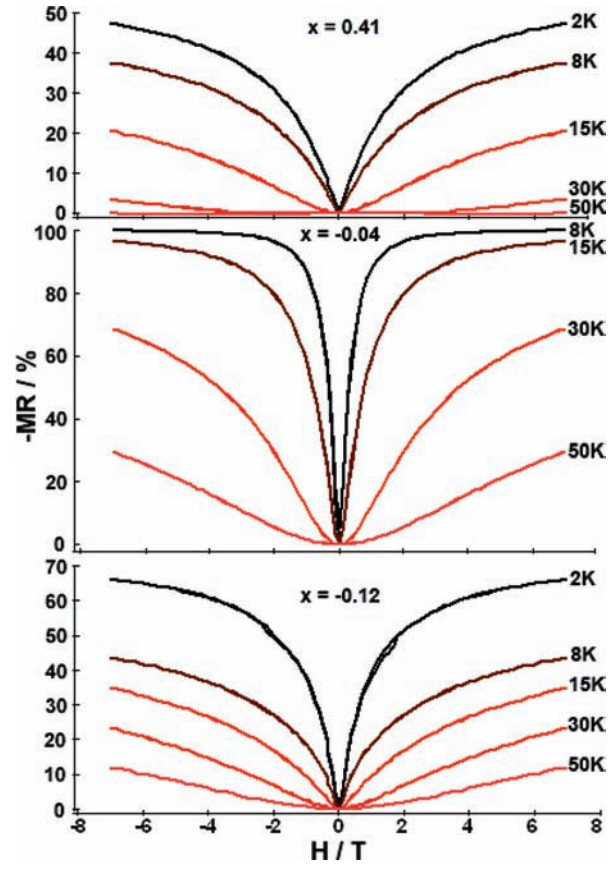

Figure 7. Magnetic-field variations of negative magnetoresistances ($-MR = (\rho_0 - \rho_H)/\rho_0$) for $EuWO_{1+x}N_{2-x}$ ($x = 0.41$, -0.04, and -0.12).

(20) Katsufuji, T.; Takagi, H. *Phys. Rev. B* **2001**, *64*, 054415.

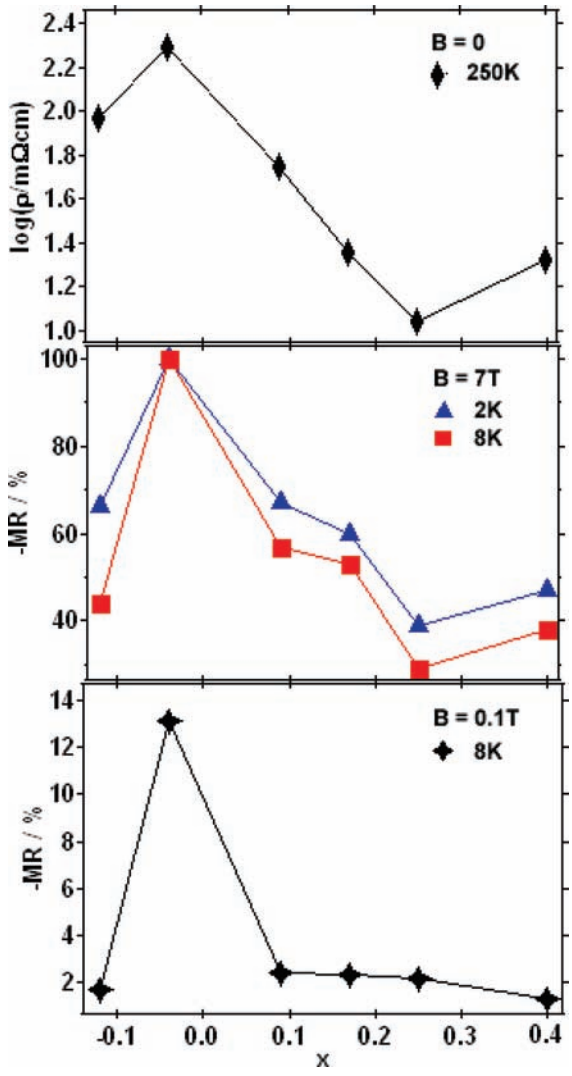

Figure 8. Compositional variations for $EuWO_{1+x}N_{2-x}$ of 250 K resistivity, high-field (7 T) magnetoresistances at 2 and 8 K, and low-field (0.1 T) magnetoresistance at 8 K.

T field, as the zero-field resistance was too high to be measured accurately at lower temperatures. Hence, $EuWO_{1+x}N_{2-x}$ is found to be a new CMR material at low temperatures, for dopings x close to zero (here $x = -0.04$).

Resistivity data for the three $EuWO_{1+x}N_{2-x}$ samples measured here ($x = 0.41$, -0.04, and -0.12) and those for three previous electron-doped samples ($x = 0.25$, 0.18, and 0.09) are combined to show overall trends in Figure 8. The highest resistivities and the strongest temperature dependence are observed for the $x = -0.04$ sample, which confirms that minimum doping occurs close to the ideal $x = 0$ composition. The bandgap for the $x = -0.04$ sample estimated from the slope of log(resistivity) at room temperature is 60 meV, showing that the $EuWO_{1+x}N_{2-x}$ materials have narrow bandgaps. The hole-doped $x = -0.12$ material has a higher resistivity than samples with comparable magnitudes of electron doping ($x = 0.09$ and 0.17). This is in keeping with the expected carrier mobilities, as f-band holes are expected to be less mobile than the 5d-band electrons; that is, $Eu^{2+}-Eu^{3+}$ electron transfer is less rapid than $W^{5+}-W^{6+}$ transfer. Resistivity decreases as hole or electron doping increases, although the $x = 0.41$ material has an anomalously high resistivity that may reflect some electrical inhomogeneity close to the upper limit of nitrogen deficiency.

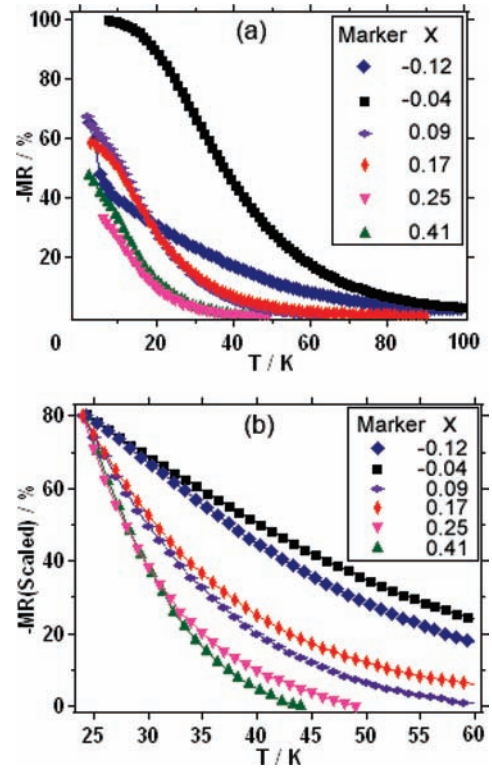

Figure 9. Temperature variations of the 7 T magnetoresistances for $EuWO_{1+x}N_{2-x}$ samples, (a) showing $-$MR values below 100 K and (b) scaled to the 24 K value for the $x = -0.04$ sample ($-$MR = 80%) to compare the variations in the paramagnetic regime.

The compositional trends in low-temperature magnetoresistance follow the resistivity variations, as illustrated by Figure 9. The most resistive $x = -0.04$ sample is the only one to show a CMR effect in high fields. This material also shows a very rapid rise in $-$MR at low fields. The low-field (0.1 T) value of $-$MR is 13% for the latter sample at 8 K but <3% for all other samples. Low-field magnetoresistances of ceramic materials are often dominated by the magnetotransport of carriers across the boundaries between different grains or magnetic domains. These effects are more dependent on sample microstructure than composition and so do not follow simple chemical trends. Hence the observed variation strongly indicates that the low-field magnetoresistance is intrinsic to the $EuWO_{1+x}N_{2-x}$ materials rather than of microstructural origin. This also demonstrates that the intrinsic electronic properties of the "undoped" $x = 0$ material are apparent despite any additional carriers introduced by anion disorder.

Figure 9 shows that $-$MR increases on cooling in the paramagnetic region for all of the $EuWO_{1+x}N_{2-x}$ materials, and only for the $x = -0.12$ sample is there evidence for a specific increase below T_C that may indicate a tunneling magnetoresistance across grain or domain boundaries. The majority of behavior shows that $-$MR is dependent primarily on field-induced changes in local magnetization, which are substantial for an $S = 7/2$ paramagnet at low temperatures. The $x = -0.04$ material that shows CMR effects below T_C also shows substantial magnetoresistance in the paramagnetic regime, e.g., $-$MR = 25% at 60 K ($= 5T_C$). This is attributed to the magnetotransport mechanism specific to holes as discussed below.

The large negative magnetoresistances of the electron-doped materials $EuNbO_2N$ and $EuWO_{1+x}N_{2-x}$ ($x > 0$) arise from the coupling of the transition metal d-band carriers to those of the

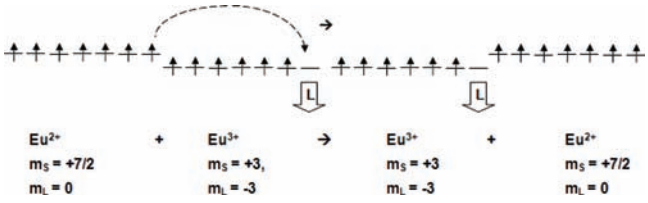

Figure 10. Schematic illustration for the double exchange between Eu^{2+} ($4f^7$) and Eu^{3+} ($4f^6$) configurations, leading to parallel alignment of the spin angular momenta (m_S; individual electron spins shown as thin upright arrows), and hence order of the Eu^{3+} orbital angular momenta (m_L; block arrows) in the opposite direction.

localized Eu^{2+} $S = 7/2$ spins. This is comparable to the double exchange picture for manganites, where the motion of an e_g electron between Mn^{3+} and Mn^{4+} ions is favored by the parallel alignment of their $S = 3/2$ spin cores. In the electron-doped $EuWO_{1+x}N_{2-x}$ perovskites, the core spins are from $S = 7/2$ Eu^{2+}, while the carriers are the W d-band electrons resulting from the reduction of W^{6+} to W^{5+}. This is similar to the mechanism for large magnetoresistances in n-type europium(II) oxide samples, EuO_{1-x}, where the transport of sp-band electrons introduced by doping with excess Eu is coupled to the ferromagnetic order of the Eu^{2+} spins.[21]

The observation of large negative magnetoresistances for the hole-doped $EuWO_{1+x}N_{2-x}$ ($x < 0$) materials shows that the hopping of Eu 4f-band holes between Eu^{2+} and Eu^{3+} ions is also highly spin-polarized. This is analogous to the double exchange mechanism for Mn^{3+}/Mn^{4+} hopping, but with the additional consequence that the 4f hole hopping also polarizes the $L = 3$ orbital angular momentum antiparallel to the $S = 3$ spin momentum for the $J = 0$ ground state of the Eu^{3+} configuration, as these are Hund's-rule coupled, as shown in Figure 10. An interesting possibility that this raises would be a spin-polarized Eu^{3+} analogue of the "half-metallic antiferromagnet" scenario (more correctly, a spin-polarized compensated ferrimagnet) where conduction electron spins are polarized in a material with near-zero net magnetization. This can be realized in double perovskites such as Sr_2CrMO_6 (M = Ru, Os) when the Cr and M ions are ordered, as their spins (intermediate between $S = 3/2$ for Cr^{3+}/M^{5+} states and $S = 1$ for Cr^{4+}/M^{4+}) are opposed but only one carrier spin direction is favored.[22,23] Double exchange in a lightly doped Eu^{3+} material could result in parallel alignment of all Eu^{3+} $S = 3$ spin moments, resulting in the opposite orientation for all Eu^{3+} $L = 3$ orbital moments at low temperatures when only the $J = L - S = 0$ ground state is populated (Figure 10). Hence, a spin-polarized current would flow in a material where most ions had a $J = 0$ ground state.

A difference between the magnetotransport mechanisms of the electron- and hole-doped materials is evident from the temperature variations of high-field magnetoresistance shown in Figure 9. The two hole-doped samples ($x = -0.04$ and -0.12) have magnetoresistances that decline more gradually with temperature above T_C than those of the electron-doped samples. This is apparent when all of the −MRs are scaled to the same value at 24 K ($= 2T_C$) for direct comparison (Figure 9b) or by comparing the 50 K −MR vs H data for the $x = -0.12$ and 0.41 samples in Figure 7. Magnetoresistance varies with magnetization approximately as $-MR \sim M^2$, but as the hole-doped samples have smaller Curie constants (Table 3) and hence magnetizations than the electron-doped materials, magnetization differences do not account for the larger −MRs of the former. Instead, this effect reveals the different extents of spin−spin correlation that are required for transport in the two doping regimes.

The probability of a carrier hopping between two sites i and j is proportional to $\underline{M}_i \cdot \underline{M}_j$ where $\underline{M}_i$ and $\underline{M}_j$ are the magnetizations at the two sites. The f-band holes hop directly between the localized spins on the Eu ions, as shown in Figure 10, so the site magnetizations are dominated by the Eu spins present. Hence, the increase in local correlations between pairs of adjacent Eu^{2+} and Eu^{3+} spins when a magnetic field is applied leads to an increase in hole transport. However, in the electron-doped materials the d-band carriers hop between nonmagnetic W ions, and the site magnetizations arise from the alignments between nearby Eu^{2+} spins. In the cubic perovskite structure, the closest spins to each W ion are from eight Eu ions, four of which are shared with the neighboring W ion. Thus, correlations between a cluster of ~12 local spins are needed to increase the rate of electron hopping between neighboring W^{5+} and W^{6+} ions. At temperatures $T \gg T_C$, such multispin correlations are less easily induced by a magnetic field than two-spin correlations, and hence the magnetotransport of W d-electrons is much smaller than that of Eu f-holes.

Conclusions

$Eu_2W_2O_9$ is transformed into $EuWO_{1+x}N_{2-x}$ perovskites under ammonolysis conditions through two chemical transformations accompanied by structural rearrangements. The initial step is an almost pure reduction to the scheelite-type intermediate $EuWO_{4-y}N_y$, which is slightly nitrided with maximum $y \approx 0.04$. The second stage is essentially a substitution of oxide by nitride to yield the perovskite, but additional reduction or oxidation can occur, enabling a wide range of $EuWO_{1+x}N_{2-x}$ materials ($-0.16 < x < 0.46$ in this study) to be accessed by varying the reaction time, temperature, or ammonia flow rate. The ideal $x = 0$ composition does not appear to have any specific kinetic or thermodynamic stability.

The synthesis of $EuWO_{1+x}N_{2-x}$ materials with both negative and positive x values is significant, as it demonstrates that the oxidation states of two different metals may be controlled through variation of the O/N ratio in the perovskite structure type. This is in contrast with typical oxide perovskites, where the ratio of fixed valence cations at one site is used to tune the oxidation state at the other, e.g., the CMR materials $La_{1-x}Sr_xMnO_3$. This electronic tunability is of particular interest, as in principle it enables $EuWO_{1+x}N_{2-x}$ to behave as an n-type semiconductor through electron doping of the W: $5d(t_{2g})$ band) for $x > 0$, or as a p-type material with conduction by 4f-band holes for negative x. Hence, a p−n junction could be fabricated from this material by controlling the spatial variation of O/N content. The variation of resistivity with x confirms this electronic bifunctionality, as the most resistive sample has the smallest $|x|$ value ($x = -0.04$).

Anion disorder tends to introduce additional holes (Eu^{3+} states) and electrons, reducing the magnetic moments from the expected Eu^{2+} values, although this has not obscured the intrinsic properties of the least-doped $x = -0.04$ material. The electronic properties of $EuWO_{1+x}N_{2-x}$ are thus controlled both by the compositional variable x, which determines the numbers

(21) Shapira, Y.; Foner, S.; Reed, T. B. *Phys. Rev. B* **1973**, *8*, 2299.
(22) Krockenberger, Y.; Mogare, K.; Reehuis, M.; Tovar, M.; Jansen, M.; Vaitheeswaran, G.; Kanchana, V.; Bultmark, F.; Delin, A.; Wilhelm, F.; Rogalev, A.; Winkler, A.; Alff, L. *Phys. Rev. B* **2007**, *75*, 020404(R).
(23) Rodgers, J. A.; Williams, A. J.; Martínez-Lope, M. J.; Alonso, J. A.; Attfield, J. P. *Chem. Mater.* **2008**, *20*, 4797–4799.

of holes or electrons introduced by chemical doping, and by the amount of anion disorder, which controls the number of additional hole−electron pairs created. A future challenge will be to measure the degree of anion order using neutron diffraction and perhaps local probes and to relate this to the physical properties at a given x. Ultimately this could enable both disorder and composition tuning of the physical properties.

The low-temperature ferromagnetism of $EuWO_{1+x}N_{2-x}$ materials leads to spin polarization of the carriers and magnetic semiconductor behavior resulting in large negative magnetoresistances, with CMR observed near $x = 0$. Hole magnetotransport results from a double exchange between Eu^{2+} and Eu^{3+} states that should lead to polarization of the Eu^{3+} spin and orbital angular momenta, despite their overall cancellation in the $J = 0$ ground state. This double-exchange model is corroborated by the observed large magnetoresistances of the hole-doped materials in the paramagnetic regime, reflecting the lower levels of spin correlation required for magnetotransport in comparison to the electron-doped materials.

Acknowledgment. This work was supported by the Ministerio de Ciencia e Innovación (grants MAT2008-04587 and PR2008-0164) and the Generalitat de Catalunya, Spain, and EPSRC, the Royal Society, EaStCHEM, and the Leverhulme Trust, U.K.

Supporting Information Available: This material is available free of charge via the Internet at http://pubs.acs.org.

JA910745B